Different Fermi-level pinning positions between epitaxial and rotational Al/Si interfaces

Y. Miura, S. Fujieda, and K. Hirose
Microelectronics Research Laboratories, NEC Corporation, 34 Miyukigaoka, Tsukuba, Ibaraki 305, Japan
(Received 20 July 1993; revised manuscript received 21 March 1994)

Schottky-barrier height (SBH) for intimate Al/Si contacts is investigated in relation to the interfacial crystallographic alignment, which is observed by transmission-electron microscopy. Epitaxial and rotational Al films are obtained by low-temperature molecular-beam epitaxy on both Si(111) and (100) surfaces, by controlling the surface structures. The SBH measurements for *n*- and *p*-type samples reveal that the absence of epitaxial alignment at the interfaces significantly lowers the Fermi-level pinning position for the contacts on both (111) and (100) surfaces.

Schottky-barrier formation at Al/Si interfaces has been studied extensively because such interfaces have been utilized as typical contacts in Si devices. Theoretical studies on the Fermi-level (FL) pinning mechanism has also been developed based on this model system,[1-3] which is chemically inactive and makes no silicide bonds. However, the reported Schottky-barrier height (SBH) is not unique and scatters widely over the range of 0.66–0.77 eV, even when limited to intimate contacts on *n*-type Si(111) surfaces.[4-9] This variation is too large to be explained only by experimental errors. However, in most previous studies, the origin of the scattered SBH's has not been clarified. Thus, it is necessary to determine the barrier heights for the Schottky contacts, the interfacial structures of which are well characterized.

Recently, epitaxial Al(111) films have been grown on Si(111) substrates by Al evaporation in ultrahigh vacuum.[9-11] Furthermore, we have succeeded in growing single-phase epitaxial Al(111) films on Si(111) substrates by using low-temperature molecular-beam epitaxy (MBE) without post-growth annealing.[12] For such contacts, the SBH is expected to be defined uniquely. We have also obtained polycrystalline films with rotational (111)-textured grains, merely by controlling the Si(111) surface structures.[12] In the same way, on (100)-oriented surfaces, two types of contacts with epitaxial and rotational grains have been formed. Fabrication of such well-characterized contacts enables us to investigate the cause of the SBH variation. In this paper, we describe *n*- and *p*-type SBH's and the interfacial crystallographic alignment, for intimate Al contacts on Si(111) and Si(100). It is shown that the FL pinning position for nonepitaxial interfaces is lower than that for the epitaxial interfaces.

The substrate preparation is the critical process in this experiment. The substrates used were (111)- and (100)-oriented *n*- and *p*-type Si wafers with resistivities of 10–20 Ω cm. All the substrates were hydrogen terminated by being dipped into *p*H-controlled HF solutions for 60 s; *p*H=8 for the Si(111)-oriented wafers and *p*H=4 for the Si(100)-oriented wafers. They were immediately loaded into an MBE chamber with a base pressure of less than 1×10^{-10} Torr. The Si(111) surfaces were mainly terminated by silicon-monohydride bonds and the Si(100) surfaces by silicon-dihydride bonds.[13,14] Both surfaces showed 1×1 reflection high-energy electron diffraction (RHEED) patterns. In addition to these hydrogen-terminated (111) and (100) surfaces, three kinds of *in situ* cleaned surfaces were prepared by annealing the starting hydrogen-terminated surfaces (Table I). After thermal treatment of 800 and 600 °C (Ref. 15) for 10 min, the Si(111) surfaces showed RHEED patterns of 7×7 and 1×1, respectively. On the latter surface, the surface reconstruction is thought to be incomplete or disordered. The Si(100) treated at 700 °C for 10 min showed a 2×1 pattern. These thermally treated surfaces are considered to be hydrogen-free because the hydrogen atoms terminating the surface desorb at 530 °C.[16] After reaching the maximum temperature, the pressure was kept at no more than 1×10^{-9} Torr. During sample cooling and subsequent Al growth, the ion gauge was switched off to minimize the ambient effect on the surfaces.[17] Then Al was evaporated onto these oxide-free surfaces from an effusion cell at a substrate temperature of 50 °C. The growth rate was set at 0.04 nm/s and the film thickness at about 60 nm. All Al films had flat mirror surfaces. No post annealing was performed in this study.

The structures of the Al films were analyzed by transmission electron microscopy (TEM) using a JEOL JEM-4000EX. The samples were thinned by mechanical polishing and Ar-ion milling on the Si side. The overlap region of the Al and Si layers was observed by plan-view TEM. The transmission electron diffraction (TED) patterns are shown in Figs. 1(a)–1(c) for the three samples on the Si(111) substrates, and are shown in Figs. 1(d) and 1(e) for the two samples on the Si(100) substrates. These five samples are denoted samples *A*–*E*, as shown in Table I, where the observed crystallographic relations between Al and Si are summarized.

TABLE I. Structures of Al films grown on various Si(111) and Si(100) surfaces prepared by different *in situ* treatments. The Si surface structures before Al evaporation were identified by RHEED patterns. The crystallographic structures of Al films were determined by TEM observation.

Sample	Si surface	Al film
A	(111):7×7	epitaxial-(111)
B	(111):1×1	rotational-(111)
C	(111):1×1(-*H*)	epitaxial-(111)+(100)
D	(100):2×1	epitaxial-(110)
E	(100):1×1(-*H*)	rotational-(110)

 ©1994 The American Physical Society

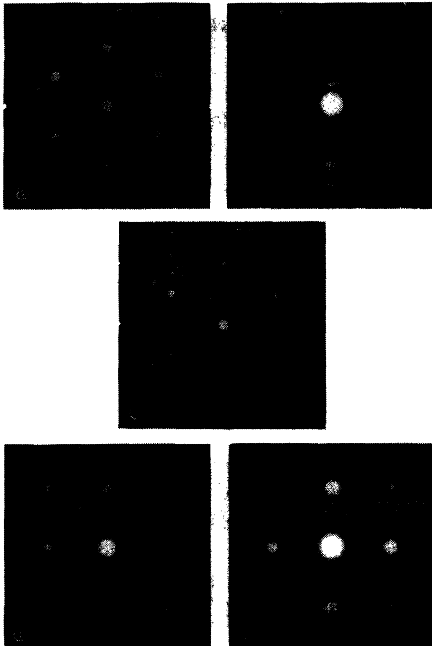

FIG. 1. Plan-view TED patterns from the overlap region of Al and Si layers for the samples on (111)- and (100)-oriented substrates. Here, (a)–(e) represent the TED patterns of samples *A*–*E*, respectively. *S*, *A*1, *A*2, and *A*3 indicate the diffraction spots of Si(220), Al(220), Al(200), and Al(111), respectively. The spots of *D*1, *D*2, and *D*3 are caused by double diffraction at the Al and Si layers, corresponding to the spots of *A*1, *A*2, and *A*3.

Figure 1(a) shows a perfect epitaxial relation in sample *A*: Al(111)||Si(111) with Al⟨220⟩||Si⟨220⟩. Furthermore, cross-sectional TEM observation revealed that the films have only type-A orientation. The TED pattern for sample *B* in Fig. 1(b) shows that the Al film is (111) oriented. However, Al diffraction spots appear as arcs at an angle of ±10° around the regular epitaxial diffraction spot positions. This means that the Al films consist of grains rotating with random angle distribution in the plane parallel to the interface. The mean grain size was 50 nm in the TEM images. The TED pattern for sample *C* in Fig. 1(c) shows that the Al film consists of two kinds of grains with the following epitaxial relations to the Si substrate: Al(111)||Si(111) with Al⟨220⟩||Si⟨220⟩, and Al(100)||Si(111) with Al⟨220⟩||Si⟨220⟩. The mean grain size was 100–200 nm.

The TED pattern of Fig. 1(d) shows that the Al film for sample *D* is a bicrystal consisting of two equivalent epitaxial grains: Al(110)||Si(100) with Al⟨220⟩||Si⟨220⟩. Figure 1(e) shows that the Al film is (110) oriented, but the grains are rotated (±10°) around the two epitaxial orientations with random angle distribution, as in the case of sample *B*. The mean grain sizes for both samples *D* and *E* were 100–200 nm.

As revealed by plan-view TEM observations, the main difference in the film structure is the presence or absence of grain rotation around the normal axis. Cross-sectional TEM observation has shown that the polycrystalline Al films have columnar structure and that the crystallographic orientation of the metal film is extrapolated to the very interface. The epitaxial samples on both (111) and (100) substrates have common epitaxial relations along the ⟨220⟩ directions in the interfacial plane, where the ratio of the lattice constant of Si to that of Al can be well approximated by the simple rational number $\frac{4}{3}$, with a small mismatch of 0.6%.

The SBH's of the above five samples on the *n*-type Si were determined by current voltage (*I*-*V*), 1-MHz capacitance-voltage (*C*-*V*), and internal photoemission (IPE) measurements[18,19] at 300 K. For the electrical measurements, Ohmic contact was made on the back side of the sample after scratching off the oxide layer. Arrays of Schottky diodes, 500 μm in diameter, were fabricated by Au/Ti deposition on the Al film through a stainless-steel mask and subsequent etching in H_3PO_4 to define the diodes. In the IPE measurement, infrared light from a double monochromator was incident on the back sides of the diodes. A Richardson constant of 112 $A\,K^{-2}\,cm^{-2}$ was used for *I*-*V* analysis. For each sample, SBH's were measured for several diodes fabricated from different parts of the wafer. The average SBH's are summarized in Table II. The values for each sample ranged within ±10 meV for *I*-*V* and *C*-*V* measurements, and within ±15 meV for IPE measurement.

Figures 2(a) and 2(b) show typical sets of forward current characteristics in *I*-*V* measurement for (111) and (100) substrates, respectively. For all ln*I*-*V* plots, good linearity is observed over two orders of magnitude in current. The ideality factor *n* of each diode in the ln*I*-*V* plot of each diode was close to unity ($1.01 \le n \le 1.05$) independent of the samples. These results indicate that none of the extrapolated SBH values are affected very much by recombination current,[18] which is caused by disorder or defects near the interface. The $1/C^2$-*V* plot also showed excellent linearity and gave a doping concentration of $N_d = 4.0 \times 10^{14}$ cm^{-3} for each sample. This corresponds to the nominal resistivity of the *n*-type substrates. The SBH (*C*-*V*) data are quite similar to the SBH (*I*-*V*) data, as shown in Table II. Figures 3(a) and 3(b) show typical sets of IPE spectra for (111) and (100) substrates, respectively. Each Fowler plot[19] ($Y^{1/2}$-$h\nu$) was found to be linear over the range of photon energy $\phi+3$ kT $< h\nu < 0.98$ eV, where Y and ϕ are the quantum photoelectric yield and the intercept of the plots with the $h\nu$ axis, respectively. The photoelectric yield in this photon energy region is normalized by the yield at the photon energy of 1.1–1.2 eV, where electron-hole generation in bulk Si is dominant. The SBH's are determined as the intercepts ϕ of the Fowler plots. As shown in Table II, the

TABLE II. SBH's for Al contacts on *n*-type Si substrates. Barrier height values, $\phi_{Bn}(I\text{-}V)$, $\phi_{Bn}(C\text{-}V)$, and $\phi_{Bn}(\text{IPE})$, were determined by current-voltage, capacitance-voltage, and internal photoemission methods, respectively, at 300 K.

Sample	$\phi_{Bn}(I\text{-}V)$ (eV)	$\phi_{Bn}(C\text{-}V)$ (eV)	$\phi_{Bn}(\text{IPE})$ (eV)
A	0.68	0.69	0.69
B	0.75	0.77	0.75
C	0.69	0.69	0.71
D	0.70	0.71	0.70
E	0.76	0.78	0.77

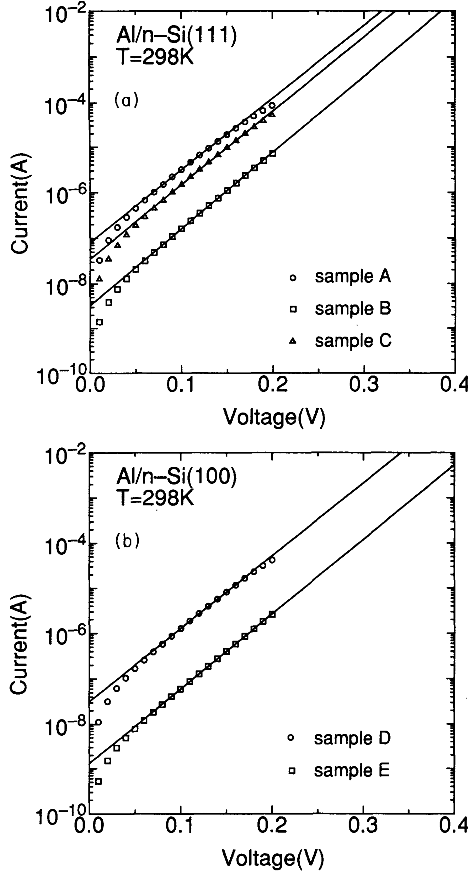

FIG. 2. Typical sets of forward current characteristics in $\ln I$-V plots for the contacts on (111)-oriented surfaces (a) and (100)-oriented surfaces (b), respectively. The contact area is 1.9×10^{-3} cm^{-2}. The SBH's were determined from the saturation current, which is extrapolated by fitting the plots in the bias range of 80–180 meV.

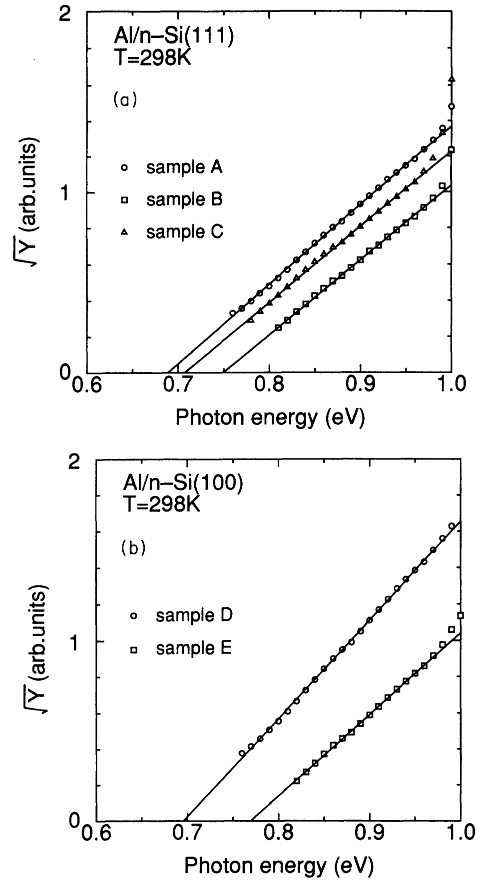

FIG. 3. Typical sets of IPE spectra in Fowler plots for the contacts on (111)-oriented surfaces (a) and (100)-oriented surfaces (b), respectively. The SBH's were determined as threshold photon energy, which is extrapolated by fitting in the range of $\phi+3\,\mathrm{kT}<h\nu<0.98$ eV.

SBH's of the five samples agree well with the corresponding SBH's determined by I-V and C-V methods. These results confirm the accuracy of the SBH values because the photoelectric measurement is a direct method of determining the barrier height without any external parameters.[5,19] The SBH differences among samples are as much as 70 meV, which is significantly larger than the precision of each measurement.

The p-type SBH's were determined by the C-V method at 200 K because of the difficulty in determining the low ϕ_{Bp} (≤ 0.5 eV) at room temperature. The n-type Si SBH's were also measured at 200 K. Hereafter, the SBH's for the n- and p-type substrates will be referred to as ϕ_{Bn} and ϕ_{Bp}, respectively. The results are listed in Table III. Each SBH value is the average over several diodes, and the values for each sample are within the range of ±10 and ±15 meV for n- and p-type samples, respectively. For each p-type diode, good linearity in the $1/C^2$-V plots was observed, at least for reverse applied voltage of less than 0.5 V. The obtained dopant concentration of $N_a=1.1\times10^{15}$ cm^{-3} corresponds to the nominal substrate resistivity mentioned above. For the n-type samples, the $1/C^2$-V plots showed excellent linearity and reproduced an SBH difference of 70 meV observed at 300 K. Notice that ϕ_{Bn} and ϕ_{Bp} for each sample change complementarily depending on the film structures. All the values of $\phi_{Bn}+\phi_{Bp}$ listed in Table III are nearly equal to the Si band gap E_g ($=1.15$ eV) at 200 K. This result suggests that the SBH differences among samples essentially reflect the differences in FL pinning positions.

Before discussing the variation of the FL pinning position, we have to examine the effect of SBH inhomogeneity,[20] which may affect the apparent SBH. The present samples except for sample A evidently have inhomogeneous interface structures. However, the n-type samples showed no distinctive signs of SBH inhomogeneity; SBH's (I-V) determined with a rather good ideality factor agree well with the SBH's determined by C-V and

TABLE III. SBH's on n- and p-type substrates. Barrier height values ϕ_{Bn} and ϕ_{Bp} were determined by capacitance-voltage method at 200 K.

Sample	ϕ_{Bn} (eV)	ϕ_{Bp} (eV)	$\phi_{Bn}+\phi_{Bp}$ (eV)
A	0.68	0.43	1.11
B	0.77	0.34	1.11
C	0.71	0.41	1.12
D	0.72	0.41	1.13
E	0.79	0.36	1.15

IPE measurements. This can be explained by considering the screening length. A low barrier height region, if any, would be almost pinched off[20] on the present low-doped substrates (4×10^{14} cm^{-3} for n-type Si), the Debye length (200 nm) of which is greater than or comparable to the grain sizes. Therefore, the apparent SBH's by three methods should be approximately equal to the arithmetic average of the local SBH. Although the SBH values are spatially averaged, the SBH variation still reflects characteristic differences at the Al/Si interface.

The SBH's for sample A are believed to be representative of the epitaxial Al(111)/Si(111) contacts. The value of $E_c - E_f = 0.68-0.69$ eV for sample A gives the intrinsic FL pinning position for this contact, which is located rather high in the range of the previously reported values[4-9] for intimate contacts on Si(111). The FL pinning position for another epitaxial contact on Si(111) (sample C) is close to that for sample A. This good agreement is a bit unexpected when we consider the fact that sample C contains (100)-oriented epitaxial grains in addition to (111) epitaxial grains. On the other hand, the FL pinning position for the nonepitaxial contacts with rotational grains (sample B) is lower by as much as 70 meV than that for sample A, even though Al films of both samples are completely (111) oriented. Similar SBH dependence on the crystallographic orientation also holds for the contacts on the Si(100) surfaces. The FL pinning position for the nonepitaxial contacts (sample E) is lower by as much as 70 meV than that for the epitaxial contacts (sample D). This difference is also marked because the Al films for both samples have common (110) orientation and the same grain size. Here, the absolute SBH values of (111) and (100) contacts cannot be compared directly because the difference in surface atom density significantly affects the SBH. However, these results clearly indicate that the absence of epitaxial alignment at the interfaces significantly lowers the FL pinning position for the contacts on both (111) and (100) substrates. It should be noted that the difference in FL pinning positions cannot be consistently explained by extrinsic factors, such as the temperature of *in situ* thermal pretreatment of the wafers, or by the presence of hydrogen on the surface just before metallization.

Finally, we comment on the interfacial structure at the Al/Si interfaces. It has been established that the SBH strongly depends on the atomic interfacial structures for some intimate epitaxial Schottky contacts.[21-23] However, since the Al/Si system has a large lattice mismatch, it is difficult to define a simple ordered interfacial structure even for the epitaxial interface. It has been reported that epitaxial Al films deposited on the Si surface are completely relaxed and incommensurate.[24] For such an interface, the orientational matching at the interface is believed to affect the FL pinning position through various kinds of interfacial states, as suggested from the present study. In order to clarify the role of the orientational alignment at the interface, it is necessary to reveal the microscopic characteristics of the interfacial geometries.

In summary, it was found that SBH of Al/Si interfaces depends on the crystallographic alignment of Al films fabricated by low-temperature MBE on both Si(111) and Si(100) substrates. Measurement of n- and p-type SBH's revealed that the FL pinning position changes by as much as 70 meV, depending on whether or not the interfaces have epitaxial relations. These results suggest that orientational matching at the interface significantly affects the FL pinning position, even in Schottky contacts with incommensurate interfaces.

The authors are grateful to Koichi Ishida and Yoshishige Matsumoto for their continuous encouragement.

---

[1]S. G. Louie and M. L. Cohen, Phys. Rev. B **13**, 2461 (1976).
[2]H. I. Zhang and M. Schlüter, Phys. Rev. B **18**, 1923 (1978).
[3]G. Platero, J. A. Vergés, and F. Flores, Surf. Sci. **168**, 100 (1986).
[4]M. J. Turner and E. H. Rhoderick, Solid-State Electron. **11**, 291 (1968).
[5]A. Y. C. Yu and C. A. Mead, Solid-State Electron. **13**, 97 (1970).
[6]M. Hirose, N. Altaf, and T. Arizumi, Jpn. J. Appl. Phys. **9**, 260 (1970).
[7]P. Gutknecht and M. J. O. Strutt, Appl. Phys. Lett. **21**, 405 (1972).
[8]J. D. van Otterloo and L. J. Gerritsen, J. Appl. Phys. **49**, 723 (1978).
[9]Y. Miura, K. Hirose, K. Aizawa, N. Ikarashi, and H. Okabayashi, Appl. Phys. Lett. **61**, 1057 (1992).
[10]I. Yamada, H. Inokawa, and T. Takagi, J. Appl. Phys. **56**, 2746 (1984).
[11]F. K. LeGoues, W. Krakow, and P. S. Ho, Philos. Mag. A **53**, 833 (1986).
[12]Y. Miura, S. Fujieda, and K. Hirose, Appl. Phys. Lett. **62**, 1751 (1993).
[13]G. S. Higashi, Y. J. Chabal, G. W. Trucks, and K. Raghavachari, Appl. Phys. Lett. **56**, 656 (1990).
[14]P. Dumas, Y. J. Chabal, and P. Jacob, Surf. Sci. **269/270**, 867 (1992).
[15]The temperature of the substrate surface was monitored with a radiation thermometer, which was calibrated using the effective emissivity of the Si substrate on the sample holder at the eutectic temperature of Al/Si (577 °C).
[16]G. Shulze and M. Henzler, Surf. Sci. **124**, 336 (1983).
[17]M. Missous, E. H. Rhoderick, and K. E. Singer, J. Appl. Phys. **60**, 2439 (1986).
[18]E. H. Rhoderick and R. H. Williams, *Metal-Semiconductor Contacts*, 2nd ed. (Clarendon Press, Oxford, 1988).
[19]S. M. Sze, *Physics of Semiconductor Devices*, 2nd ed. (Wiley, New York, 1981).
[20]R. T. Tung, Phys. Rev. B **45**,13 509 (1992).
[21]R. T. Tung, Phys. Rev. Lett. **52**, 461 (1984).
[22]D. R. Heslinga, H. H. Weitering, D. P. van der Werf, T. M. Klapwijk, and T. Hibma, Phys. Rev. Lett. **64**, 1589 (1990).
[23]K. Hirose, K. Akimoto, I. Hirosawa, J. Mizuki, T. Mizutani, and J. Matsui, Phys. Rev. B **43**, 4538 (1991).
[24]T.-M. Lu, P. Bai, A. S. Yapsir, P.-H. Chang, and T. J. Shaffner, Phys. Rev. B **39**, 9584 (1989), and references therein.

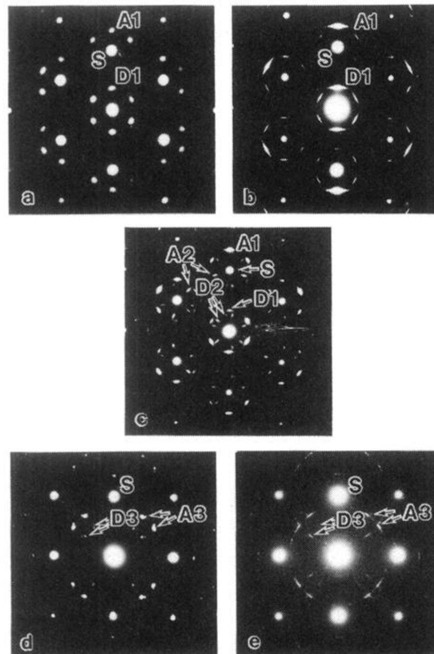

FIG. 1. Plan-view TED patterns from the overlap region of Al and Si layers for the samples on (111)- and (100)-oriented substrates. Here, (a)–(e) represent the TED patterns of samples *A*–*E*, respectively. *S*, *A* 1, *A* 2, and *A* 3 indicate the diffraction spots of Si(220), Al(220), Al(200), and Al(111), respectively. The spots of *D* 1, *D* 2, and *D* 3 are caused by double diffraction at the Al and Si layers, corresponding to the spots of *A* 1, *A* 2, and *A* 3.